Christopher Newport University

PCSE 498W - Capstone Project, Applied Physics

Development of a Monte Carlo Simulation for Electron Scattering Experiments

Author
Dillon Finkenbinder

Faculty Adviser
Dr. Peter Monaghan

April 2019

ABSTRACT

Computer simulation is one of the most effective ways to study particle scattering beyond a laboratory environment. This Capstone project was designed to simulate electron-proton scattering experiments conducted at Jefferson Lab with the High Resolution Spectrometer (HRS) via the Monte Carlo method. A Monte Carlo simulation examines the full scope of results that are possible in a scattering experiment, and replicates the stochastic nature of particle interactions by implementing a random generator.

HRS employs a suite of acceptance parameters for detecting scattered particles and their physical properties, which the simulation achieved in its development. It could then use these values to calculate physical quantities such as energy transfer, Q-squared, and Bjorken-X scaling under the acceptance conditions of the spectrometer. Simulated results were then compared to samples of experimental data through visual and statistical methods. Only two semesters were allotted to the development of the program, so it is rudimentary in nature. It does not implement a physical model that accounts for inelastic phenomena such as missing energy or missing momentum, but has successfully produced data that agrees with experimental results by employing other computational methods.

USEFUL VALUES

Symbol	Quantity	Value
α	Fine Structure Constant	$e^2/4\pi\epsilon_0\hbar c = \frac{1}{137} \approx 0.0073$
$\hbar$	Planck's Constant	$\frac{h}{2\pi} = 1.055 \cdot 10^{-34} eV \cdot s$
m_e	Electron Rest Mass	$0.511\ MeV$
m_p	Proton Rest Mass	$938.28\ MeV \approx 1{,}836 \cdot m_e$
u	Atomic Mass Unit	$931.494\ MeV/c^2$
c	Speed of Light in Vacuum	$3 \cdot 10^8\ m/s$
a_0	Bohr Radius	$5.29 \cdot 10^{-11} m$
Z	Elementary Charge	$1.602 \cdot 10^{-19} C \approx 1eV$
μ_e	Electron Magnetic Moment	$-9.285 \cdot 10^{-24} J/T$
μ_B	Bohr Magneton	$e\hbar/2m_e = 5.788 \cdot 10^{-11} MeVT^{-1}$
μ_N	Nuclear Magneton	$e\hbar/2m_p = 3.152 \cdot 10^{-14} MeVT^{-1}$
γ	Lorentz Factor	$1/\sqrt{1-(v/c)^2}$

Contents

1 Introduction **1**

2 Theory **1**

3 Methods **6**

4 Data **7**

5 Discussion and Conclusion **12**

1 Introduction

Since the 1950s, physicists have used electron scattering as the conventional method to study nuclear structure. Electrons are point-like particles that have a considerably smaller mass than their subatomic counterparts, and are consequently rendered as a useful probe for the nucleus at high energies. Given the complex nature of scattering experiments, another method to further study nuclear structure arises in computer simulation.

In short, simulations allow the user to measure complex quantities of a physical system without having to develop solutions analytically. This can be helpful for electron scattering as the individual trajectories of scattered particles are stochastic by nature and impossible to predict from theory alone. With modern computing methods, a random generator is used to simulate particle kinematics based off of a physical model in order to resemble experimental results.

For this Capstone project, the goal was to develop a simulation of elastic electron-proton interactions, analyze a variety of possible results via the Monte Carlo method, and compare them with data from Jefferson Lab. Monte Carlo simulations use the randomness of a scattering event to examine all possible outcomes within the constraints of a particle spectrometer. The simulation is programmed to operate on ROOT, which is an open-source data analysis framework that incorporates C++ libraries and object-oriented class structure.

The simulation itself also follows a detailed physical model of elastic and quasi-elastic interactions, which depend on several variables including incident beam strength, differential cross sections, spectrometer acceptances, and average scattering angles to name a few. The following sections will discuss how the project was executed over two semesters, and what results were achieved throughout its development.

2 Theory

Elastic Scattering

An elastic scattering event between an electron and a proton ($e^- p \rightarrow e^- p$) occurs when an incident electron beam collides with a solid target (a sheet of ^{12}C, for example). A given electron will then exchange its energy with a proton in the bound state via the electromagnetic interaction, and scatter at a certain angle from the target. The conventional representation of this process can be shown in the Feynman diagram below:

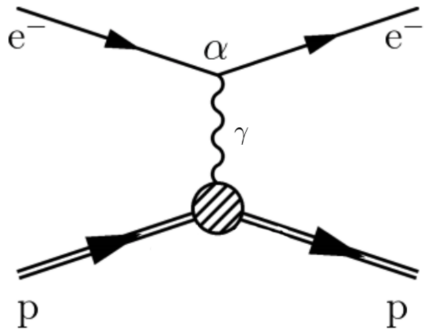

[Figure 1]

Considering that this is a high-energy collision, it is useful to introduce the relativistic conservation laws of energy and momentum. Scattering phenomena require the use of *four-vectors* to account for the kinematic behavior of particles moving close to the speed of light. Four-vectors take on the general form shown in equation (1):

$$a = (a_0, a_1, a_2, a_3) = (a_0, \mathbf{a}) \tag{1}$$

where a_0 is the relativistic or "time-like" component, and (a_1, a_2, a_3) represent the "space-like" components in *three-vector* form, written in shorthand as $\mathbf{a}$. For conservation laws in elastic scattering, the four-vector notation for momentum is given by $P = (E/c, \mathbf{p})$. E, in this case, can be written as "γmc^2" as it is the *relativistic* total energy. $\mathbf{p}$ would also be written as "γmv" to satisfy three-vector notation in a relativistic frame of reference. Thus, the conservation of four-momentum can be written as:

$$\sum_N P_i = \sum_N P_f \tag{2}$$

where N is the total number of particles. It is important to note that the scalar product between two four-vectors is *invariant*, meaning that its value will remain the same in all inertial reference frames. It is also useful to know that a particle's energy can be expressed by the energy-momentum relationship:

$$E = \sqrt{(mc^2)^2 + (pc)^2} \tag{3}$$

where mc^2 is the rest energy of the particle, and p is its momentum. These relationships will be useful later in this section when quantities like four-momentum transfer (Q^2) are derived.

In three dimensions, the trajectory of a scattered particle is usually described by a solid angle, Ω, as shown in the figure below.

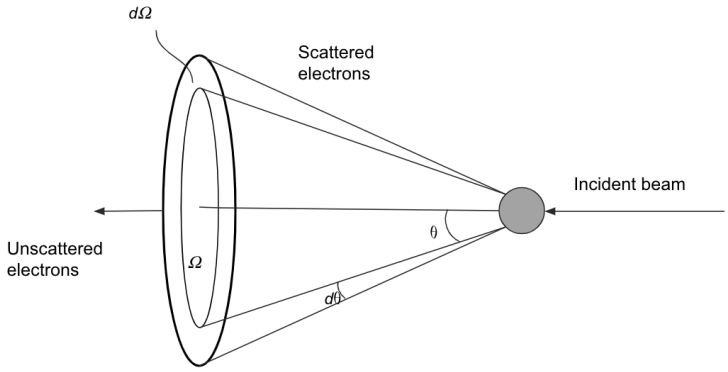

[Figure 2]

The solid angle is analogous with a spectrometer's "field of view" required to actually detect a scattered particle. Specifically, it is useful to calculate the *differential cross section* with respect to this solid angle, $\frac{d\sigma}{d\Omega}$, to determine the likelihood of a "detectable" particle interaction taking place:

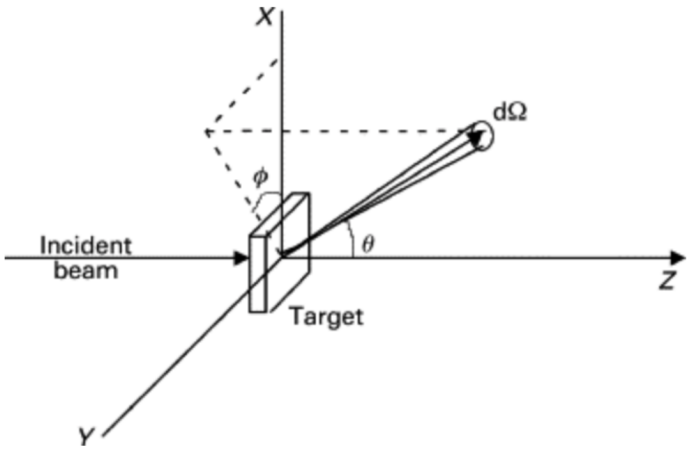

[Figure 3]

Imagine that a spectrometer is conveniently placed at the "$d\Omega$" position in Figure 3, and that the differential cross section is an expression of the *probability* that the spectrometer will detect a scattered particle in this direction. The simplest method of computing the differential cross section is to consider the interaction as completely elastic, allowing the proton to be treated as a point-like particle in the equation below:

$$(\frac{d\sigma}{d\Omega})_M = \frac{\alpha^2}{4E^2 \sin^4(\theta_e/2)} \cos^2(\theta_e/2) \tag{4}$$

where α is commonly known as the *fine structure constant* ($\approx 1/137$), E is the initial beam energy, and θ_e is the scattered angle of the electron as seen in Figure 3. This quantity is known as the *Mott Cross Section.* It is a useful calculation to make for basic scattering experiments that neglect the charge and structural properties of a nucleon. For experiments of higher energy, however, the Mott Cross Section by itself fails to represent the behavior of scattered particles. Quasi-elastic and inelastic scattering require the differential cross section to account for the proton's electromagnetic form factor, which can be described in equation (5):

$$F_P(Q^2) = \frac{1}{4\pi} \int_V \rho(\vec{r}) e^{i\vec{q}\cdot\vec{r}} \cdot d^3\vec{r} \tag{5}$$

where Q^2 is the four-momentum transfer between the two particles, $\rho(\vec{r})$ is the proton's radial charge density distribution, and $\vec{q}$ is the three-momentum transfer. Thus, the differential cross section while considering the proton's form factor can be written as:

$$\frac{d\sigma}{d\Omega} = (\frac{d\sigma}{d\Omega})_M \left| F_P(Q^2) \right|^2 \tag{6}$$

While this Capstone project does not employ physical models beyond elastic scattering, a nucleon's form factor is an important quantity to know when understanding the rationale behind probing the nucleus at high energies. The effects of these quantities are also evident in the experimental data from Jefferson Lab, which will be revisited in the discussion section.

Physical Models

Once a spectrometer successfully detects a scattered particle, there are several physical quantities that can be calculated. The simplest of them is the electron's energy transfer,

$$\omega = E - E' \tag{7}$$

where E is the initial beam energy, and E' is the scattered beam energy. In addition to energy transfer, it is also possible to account for the relativistic effects of the high-energy interaction, as seen in equations (1) - (3), by calculating the four-momentum transfer:

$$Q^2 = 4EE' \sin^2(\theta_e/2) \tag{8}$$

Considering the half-angle formula, equation (8) can also be written as $Q^2 = 2EE'(1-\cos(\theta_e))$. Some nuclear physics textbooks define the physical quantity this way.

One of the final calculations that will be relevant to this Capstone project is the Bjorken-X scaling factor. Some high-energy interactions display a unique scaling behavior during a scattering experiment that can help in determining the substructure of a nucleon, which is represented in the equation below:

$$X_B = \frac{Q^2}{2M\nu} \tag{9}$$

where M is the target mass, and $\nu = \frac{q \cdot p}{M}$ with q being the four-momentum transfer of the exchanged virtual photon and p being the incident electron's momentum. With these formulas, the next section will describe how they are used as the simulation was developed.

Particle Detection

At Jefferson Lab, a suite of electron scattering experiments are performed with the High-Resolution Spectrometer (HRS) in Hall A. HRS has two "arms" that contain different sets of particle detectors. A table of their acceptance parameters are shown below.

	$\Delta\theta$	$\Delta\phi$	δp
Electron HRS	±60mr	±30mr	±4.5%
Proton HRS	±60mr	±30mr	±4.5%

[Figure 4]

Since electrons will scatter in all directions after colliding with the target, these parameters define the "window" in which a sample of particles will be successfully detected.

3 Methods

The simulation was designed to be written and operated on ROOT, which is a data analysis framework developed by CERN. ROOT contains a rich library of C/C++ classes that are excellent in generating random events, plotting data, and analyzing results. The foundation of this project and its ability to implement the Monte Carlo method lies in the effectiveness of the random number generator and other computational methods from this framework.

To calculate the desired physical quantities for the simulation, an array of parameters were entered into a terminal prompt to set up the initial conditions of the experiment. The program would then reference these parameters while calculating each quantity, as shown in the screenshot below:

```
beam_scattered = beam_initial*cos(angle);
e_transfer = beam_initial - beam_scattered;
momentum_squared = ((4*beam_initial*beam_scattered)/C*C)*sin(angle/2)*sin(angle/2);
four_momentum = sqrt(momentum_squared);
mott_cross = (pow(FSC,2)/(4*pow(beam_initial,2)*pow(sin(angle/2),4)))*pow(cos(angle/2),2)*pow(10,-25);

p_rest = sqrt((pow(beam_initial,2)-(pow(ME,2)*pow(C,4))/(pow(C,2));
p_scattered = sqrt((pow(beam_scattered,2)-(pow(ME,2)*pow(C,4))/(pow(C,2));
px_i = p_rest*cos(angle);
py_i = p_rest*sin(angle);
px_f = p_scattered*cos(angle);
py_f = p_scattered*sin(angle);

bjorken_x = (pow(momentum_squared,2)/(2*ME*(four_momentum*p_scattered/ME)));

results.Fill();
```

(Note: not all of these variables were included in the final version of the simulation). It is easy to tell that these calculations represent the *expected* value from the given initial conditions. The next step, in this case, is to express these calculations as a distribution for "N" particles by means of random number generation.

The TRandom3 generator is a class on ROOT that uses the Mersenne Twister Algorithm to produce events. The reason why it is so useful in particle scattering simulations is because of its long period of $2^{19937} - 1$, which practically guarantees its ability to produce random numbers on par with the volume of events that may be simulated. It also has a much faster call rate in comparison to other generators like TRandom1.

Using the generator, several distributions of the kinematic and acceptance quantities could be created. To match the experimental results from Jefferson Lab, however, the simulation had to be able to discard any event that was generated outside of the spectrometer's acceptances (see Figure 4). This involved implementing a recursive generation limit that forced the program to discard events generated outside of the spectrometer's detection range, and exclusively plot the data that was produced in the allowed window. An example of this method will be shown in the next section.

The simulated data was then compared alongside the results from previous experiments in Hall A. Visually, the comparison was made by plotting both simulated and experimental data on the same histogram for both acceptance and kinematic quantities. In addition, the program determines a "goodness of fit" between the two measurements by calculating chi-squared per degree of freedom, where each bin in the histogram counts as a degree of freedom in the total calculation.

4 Data

Acceptances

As discussed in the Theory section, HRS employs a set of constraints in which a sample of scattered particles will be successfully detected. The histograms below show the "real" distributions for these constraints as defined in Figure 4 for a single experimental run.

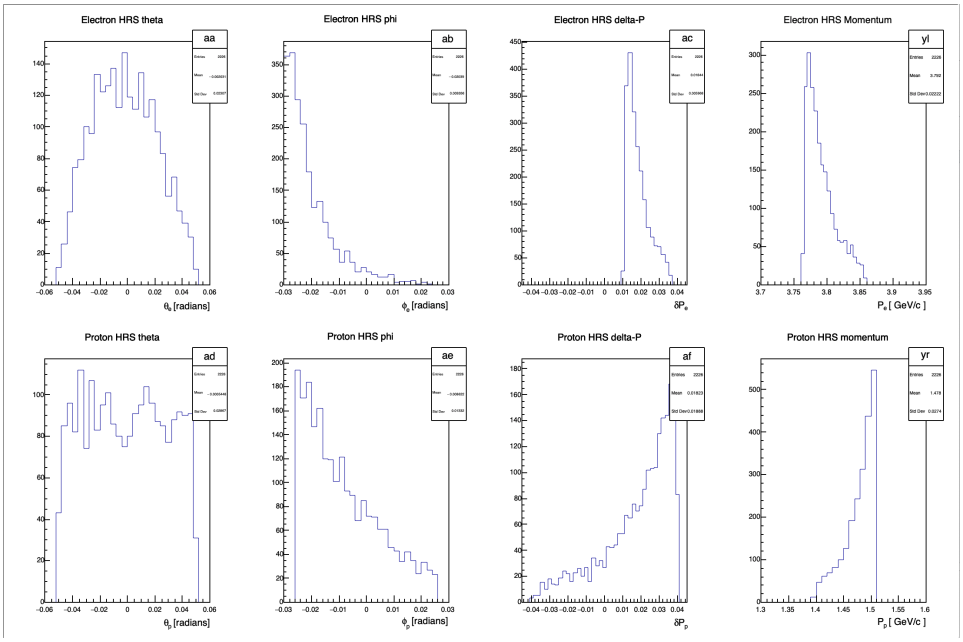

[Figure 5 - ^{12}C Target Experiment]

In reference to the numerical values in Figure 4, the successful implementation of the spectrometer's constraints is evident. In the "Electron HRS theta" histogram, for example, all detected values were plotted between ± 60mr, which agrees with the given constraints. The simulation achieved similar results to Figure 5, as shown below:

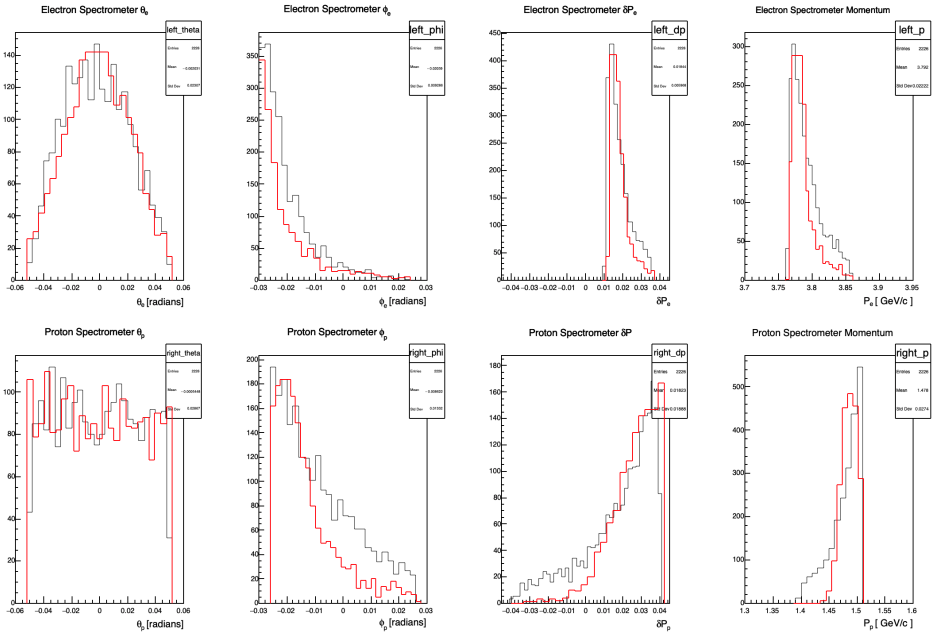

[Figure 6 - Simulation in Red]

Kinematics

To match the experimental results, the program was responsible for discarding events generated outside of the spectrometers' constraints to provide a more accurate depiction of the real data. With these results, it was possible to simulate kinematic quantities to compare with the experiment:

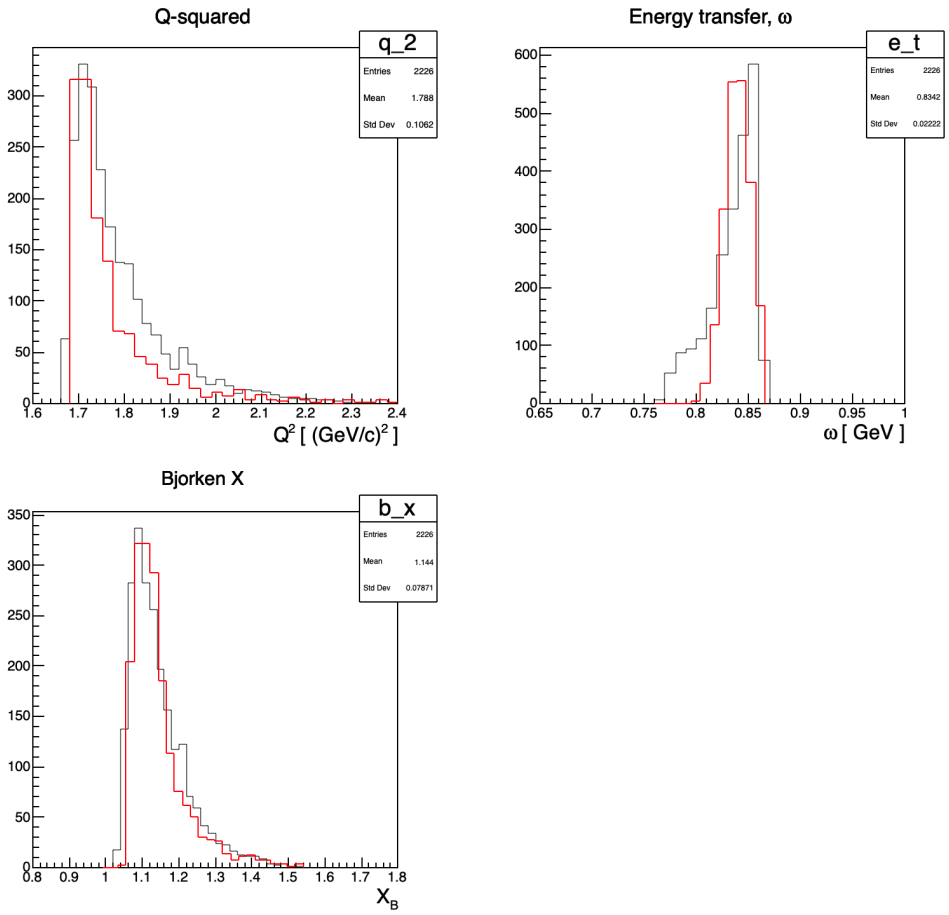

[Figure 7 - Simulation in Red]

It is useful to point out that each histogram takes on a unique shape. In the earlier stages of the simulation, the calculated quantities took the form of a uniform Gaussian distribution through the random generator; however, it was not an accurate representation of the experimental data. The latest results in Figure 6 take the form of a *Landau* distribution, which is a conventional trend for charged particles undergoing some sort of energy loss. The discussion section will elaborate on how the simulation accounted for this behavior.

Additionally, this project would not be considered a Monte Carlo simulation if it did not generate results with respect to different parameters, so Figure 7 shows a simulation of the kinematic quantities from a scattering experiment with a carbon target without cuts.

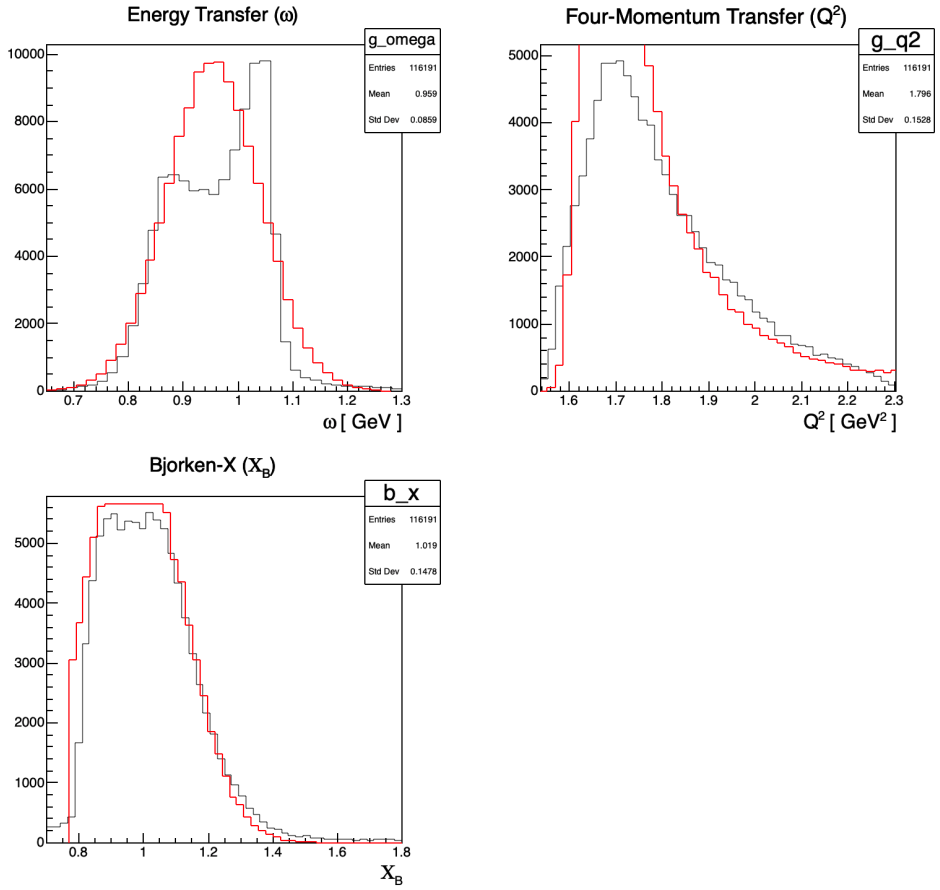

[Figure 8 - Simulation in Red]

These results are slightly different than what was expected from Figure 6. By looking at the number of entries in the gold target experiment, it is easy to tell that Figure 6 implemented a variety cuts in the data to reduce noise and other faulty results. The experiment without cuts, on the other hand, generates a set of results that look significantly different than what was found in the carbon target experiment. These discrepancies will be addressed in the discussion section.

Another goal for this project was to examine the relationship between different variables in a particle interaction, and how they change with respect to quantities like cross section and beam strength. The figure below was an attempt to fulfill this objective by using the random number generator to plot three different relationships:

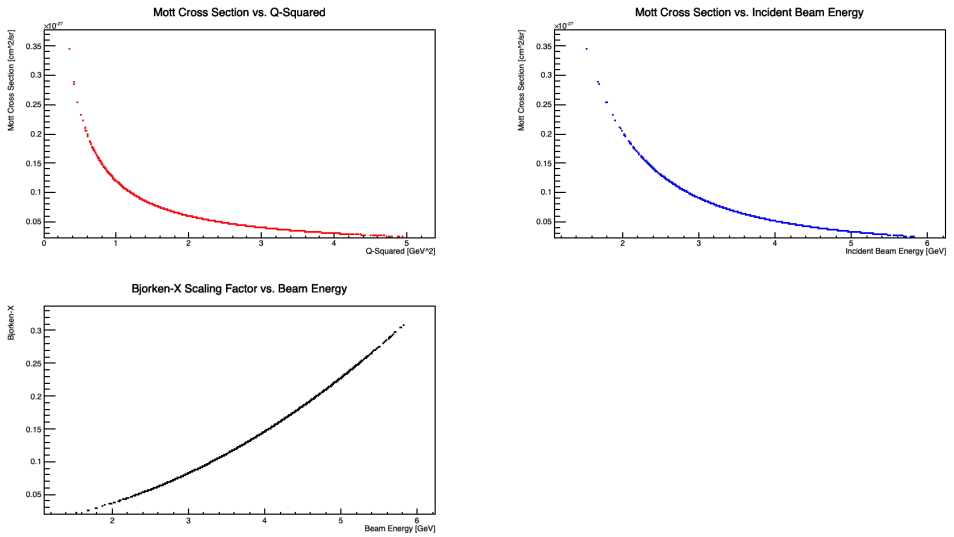

[Figure 9 - Early Simulation]

This data from earlier in the simulation was included to demonstrate how the generated values mostly adhere to the trends expected from theoretical calculations (see reference [2]), but the results are not entirely accurate. They do not account for more complex aspects of a scattering experiment, such as energy loss, to represent experimental data to the extent that earlier figures in this section were able to account for. Nevertheless, it is interesting to see how the simulation generated a set of values that conformed to a simple physical model.

5 Discussion and Conclusion

The first way to analyze the successful aspects of the simulation is to determine the "goodness of fit" between two histograms by calculating chi squared per degree of freedom. In general, this value can be expressed by equation (10):

$$\chi^2 = \frac{\sum(S-E)^2}{E} \div n \tag{10}$$

where S is the simulated value, E is the experimental value, and n is the number of bins for the histogram. Smaller values for χ^2 indicate a better correlation between the two data sets. In Figure 6, a value for χ^2/n was

calculated for each of the acceptance distributions which is shown in the following table:

Histogram Title	χ^2/n	Histogram Title	χ^2/n
Electron Spectrometer θ_e	7.621	Proton Spectrometer θ_p	9.304
Electron Spectrometer ϕ_e	3.728	Proton Spectrometer ϕ_p	22.161
Electron Spectrometer δp_e	0.780	Proton Spectrometer δp_p	0.649
Electron Spectrometer p_e	0.728	Proton Spectrometer p_p	0.518

[Figure 10 - Statistical Values for Figure 6]

Overall, these results demonstrate a general agreement between the simulation and experimental data. The ϕ_p value for the proton spectrometer, on the other hand, seems to deviate the most from experimental results. The χ^2/n results for the kinematic quantities in Figure 7 are also shown below:

Histogram Title	χ^2/n
Energy Transfer, ω	0.395
Q^2	1.934
Bjorken-X	3.312

[Figure 11 - Statistical Values for Figure 7]

These results continue to verify the agreement between simulation and experiment. Considering the rudimentary status of the program, these statistical values are better than what was originally expected. The kinematic results for the gold target experiment are shown in Figure 12:

Histogram Title	χ^2/n
Energy Transfer, ω	7.072
Q^2	1.386
Bjorken-X	3.449

[Figure 12 - Statistical Values for Figure 8]

In this case, the energy transfer calculation performed much worse than the experiment with the carbon target. This is directly correlated with the irregular shape of the histogram as seen in Figure 8. The Q^2 and Bjorken-X calculations, however, were similar to the carbon experiment and adhered to a more "uniform" distribution.

Addressing Discrepancies

It is clear in the experimental data that the measured results do not conform to a perfectly uniform curve. Some physical quantities, like ω in Figure 8, display a unique trend in the histogram. This is due to the particle interaction failing to be completely elastic. As such, the "unique" trends in the experimental histograms are a product of the energy loss behavior that occurred during an interaction.

This behavior is common for what is usually referred to as *quasi-elastic* scattering. For such interactions, there is energy lost from separating a target particle from the bound state and to release it from the nucleus. This energy loss can be quantified into variables known as *missing energy* and *missing momentum*, which were not covered in the theory section. These variables account for the energy required to separate a proton from the nucleus, as well as other unobserved energies of the residual system. This is a complex quantity to calculate, and was unfortunately beyond the scope of this project.

Despite the simulation's inability to calculate missing energy and momentum, there were other solutions to reconcile the energy loss behavior from the experiment. The random generator class on ROOT contains different methods by which distributions other than a uniform Gaussian curve

can be generated. The Bjorken-X and Q^2 values in Figures 7 and 8, for example, took the form of a *Landau* distribution. The program could then simulate this trend by calculating the physical quantity as normal, and generating the result by referencing the "Landau" function. The program was also able to read the experimental data and renormalize the histogram such that its bin contents could reach a better match. Thus, the simulated results achieved a better agreement with experimental data.

To conclude, this project has been successful in simulating electron-proton scattering experiments. Although it does not yet account for inelastic quantities like missing energy and missing momentum, there were other computational methods used to generate more realistic data. If this project were to be continued, the primary objective would be to adjust the physical models such that inelastic behavior could be accounted for. It would also be important to focus on a more broad range of scattering experiments to verify the importance of the Monte Carlo method. The source code for this project is also on GitHub, so any machine with ROOT installed will be able to use the simulation for future studies.

REFERENCES

[1] Dapor, Maurizio. "Application of the Monte Carlo Method to Electron Scattering Problems." *The European Center for Theoretical Studies in Nuclear Physics and Related Areas.* January, 2015.

[2] Griffiths, David. *Introduction to Elementary Particles.* Second Edition, Wiley-VCH, 2008.

[3] https://root.cern.ch/guides/reference-guide

[4] https://root.cern.ch/guides/users-guide

[5] Jagannatam, Archana. "Mersenne Twister - a Pseudo Random Number Generator and its Variants." George Mason University, 2010.

[6] Landau, David P. and Kurt Binder. *A Guide to Monte Carlo Simulations in Statistical Physics.* Third Edition, Cambridge University Press, 2009.

[7] Martin, B.R. *Nuclear and Particle Physics: An Introduction.* Second Edition, John Wiley and Sons Ltd, 2009.

[8] Michaels, Robert. "The Hall A Monte Carlo." *Jefferson Lab*, https://hallaweb.jlab.org. Accessed 12 March, 2018.

FURTHER READING

†Mott, N.F. and H.S. Massey. *The Theory of Atomic Collisions.* Third Edition, Oxford University Press, 1965.

†Krane, Kenneth S. *Introductory Nuclear Physics.* Third Edition, John Wiley and Sons Ltd, 1988.

†https://github.com/dfinkenbinder